Analytica Chimica Acta 1064 (2019) 94–103

Contents lists available at ScienceDirect

Analytica Chimica Acta

journal homepage: www.elsevier.com/locate/aca

Subtyping of influenza A H1N1 virus using a label-free electrochemical biosensor based on the DNA aptamer targeting the stem region of HA protein

Jyoti Bhardwaj [a], Narendra Chaudhary [a, b], Hajin Kim [a, b], Jaesung Jang [a, c, *]

[a] Department of Biomedical Engineering, Ulsan National Institute of Science and Technology (UNIST), Ulsan, 44919, Republic of Korea
[b] Center for Genomic Integrity, Institute for Basic Science, Ulsan, 44919, Republic of Korea
[c] School of Mechanical, Aerospace and Nuclear Engineering, UNIST, Ulsan, 44919, Republic of Korea

HIGHLIGHTS

- An ssDNA aptamer selected for subtyping of influenza A H1N1 viruses via SELEX is reported for the first time.
- Aptamers that recognize H1N1 subtypes alone were selected using mini HA protein and whole H1N1 viruses.
- The dissociation constant of 19.2 nM was obtained for aptamer V46.
- The electrochemical sensor based on the DNA aptamer distinguished H1N1 subtypes from other subtypes of influenza A virus.

GRAPHICAL ABSTRACT

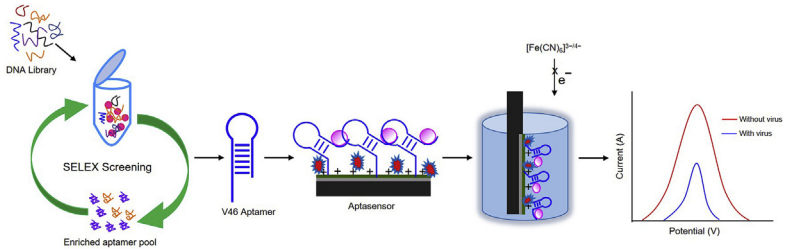

ARTICLE INFO

Article history:
Received 23 November 2018
Received in revised form
4 March 2019
Accepted 5 March 2019
Available online 9 March 2019

Keywords:
Mini-hemagglutinin (mini-HA) protein
Influenza virus
DNA aptamer
Electrochemical
SELEX
Subtyping

ABSTRACT

Rapid subtyping of influenza viruses in clinical laboratories has been increasingly important because three subtypes (seasonal H1N1, H3N2, and 2009 H1N1) of influenza A virus currently disseminated in humans have variable susceptibilities to antiviral drug. Herein, we present DNA aptamers for selective detection of influenza A H1N1 (seasonal and 2009 pandemic H1N1) viruses by targeting recombinant influenza A mini-hemagglutinin (mini-HA) protein (the stable stem region of HA) and whole H1N1 viruses. The dissociation constants (K_D) of aptamer candidates V46 and V57 were 19.2 nM and 29.6 nM, respectively, according to electrochemical characterization (differential pulse voltammetry), demonstrating strong binding to mini-HA. In comparison, the K_D of the influenza virus antibodies is in the range of 1 μM–10 nM. Aptamer V46 showed higher specificity and binding affinity to the mini-HA protein and H1N1 subtypes, and it was also incorporated into an indium tin oxide-based electrochemical sensor, showing sensitive and specific detection of H1N1 viruses, with a limit of detection (LOD) of 3.7 plaque-forming units per mL. The binding affinity, specificity, and LOD achieved with the electrochemical sensor suggest that it can be used for rapid subtyping of H1N1. We also propose that this aptamer can be used for the neutralization of H1N1 subtypes, suggesting potential therapeutic and diagnostic applications.

1. Introduction

Influenza viruses cause infections of human populations every year and are responsible for serious respiratory diseases. Influenza

* Corresponding author. School of Mechanical, Aerospace and Nuclear Engineering, Ulsan National Institute of Science and Technology (UNIST), Ulsan, 44919, Republic of Korea.
E-mail address: jjang@unist.ac.kr (J. Jang).

https://doi.org/10.1016/j.aca.2019.03.005
0003-2670/

A viruses infect a wide range of animals, including birds, swine, and other mammals; hence, they can lead to the development of pandemics [1]. Hemagglutinin (HA) and neuraminidase (NA) are the two surface glycoproteins of influenza A viruses that are the targets of immune detection. These glycoproteins are highly variable, and 18 HA and 11 NA variants have been identified thus far [2–5].

Currently, seasonal H1N1, 2009 pandemic H1N1, and H3N2 are three major subtypes disseminated in humans, and rapid subtyping in clinical laboratories is critical considering that several types of influenza viruses with variable drug resistance to antiviral treatment are cocirculating [6–8]. In fact, as of January 2010, the seasonal H1N1 viruses are known to be resistant to oseltamivir, whereas H3N2 and influenza B viruses are susceptible to oseltamivir and resistant to amantadine [9]. Currently, most commonly used methods for subtyping of influenza A viruses are based on nucleic acid specific tests such as PCR and antibody-based tests (ELISA; enzyme-linked immunosorbent assay) [6,7]. Nucleic acid-based methods are generally time-consuming, requiring trained personnel. Antibody-based subtyping is easier to perform; however, viral mutation can alter antigenic sites, which may produce pandemic viral strains, and the synthesis of new antibodies is laborious, cost-ineffective, and time-consuming [10–12].

Aptamers are chemically synthesized oligonucleotides that can recognize and bind to target molecules with high affinity and high specificity [13,14]. Their small size, low cost, and reproducible chemical synthesis, as well as flexibility for chemical modification, low immunogenicity, and lack of toxicity, make them ideal for research and diagnosis in strip tests, with considerable potential for on-site applications [15,16]. Therefore, aptamer-based subtyping would be a cost-effective and potential alternative to the antibody-based subtyping, and several DNA and RNA aptamers have been demonstrated for detection and treatment of influenza viruses (Table 1). Based on the literature, an aptamer that can distinguish the H1N1 subtype (seasonal and pandemic) from other cocirculating subtypes of the influenza virus in humans has not yet been developed.

In this study, we present a DNA aptamer with high affinity and specificity to the influenza A virus H1N1 subtype and an electrochemical aptasensor (aptamer-based biosensor) based on the developed aptamer for subtyping of influenza A H1N1 virus. Comprehensive identification of epidemic and pandemic strains of influenza H1N1 virus is challenging because of frequent viral mutations that alter surface antigens, notably on the HA protein, which is crucial for binding to the host cell prior to membrane fusion [17–19]. Previously, mini-HA proteins representing the stable HA stem (rather than the variable head) were developed from the HA sequence of the H1N1 virus (A/Brisbane/59/2007) and the crystal structure of the full-length HA of H1N1 virus (A/California/04/2009) [20]. One (#4900) of the mini-HAs provided successful protection in animal models against the influenza A group 1 heterosubtypic viruses (H1N1 A/Puerto Rico/8/34 and H5N1 A/Hong Kong/156/97) and influenza A group 2 viruses (H3 and H9 subtypes) [20]. Compared to the HA proteins that were previously used to develop DNA aptamers by several groups [21–24], the HA stem domain is much more conserved, and we postulate that targeting the stable stem region of HA, namely, mini-HA (which is not as variable as the head region), will enable the detection of all pandemic and seasonal strains of H1N1 viruses. Herein, we seek to develop ssDNA aptamers capable of detecting a broad range of influenza A H1N1 subtypes using the mini-HA protein for the first time. Our method involved the use of five rounds of systematic evolution of ligands by exponential enrichment (SELEX) with the mini-HA proteins in native active conformation, to select for the broad detection of influenza A group 1 viruses, followed by six rounds of SELEX with H1N1 viruses, to select H1N1-specific aptamers. We also developed an ITO/glass-based electrochemical aptasensor using the developed aptamer, and the aptasensor was tested against six strains of H1N1 viruses, two strains of H3N2 viruses, adenovirus virus, influenza B virus, and HA proteins of four different subtypes of influenza A viruses (H5N1, H1N2, H1N3, and H1N8).

2. Methods

2.1. Mini-HA plasmid construction, expression, and protein purification

The DNA fragment for mini-HA (#4900) protein was chemically synthesized with gBLOCK gene fragments (Integrated DNA Technologies, Coralville, IA, USA), amplified by PCR using a Phusion

Table 1
Several reported RNA and DNA aptamers for the influenza virus. HA, hemagglutinin; SPR, surface plasmon resonance; ELAA, enzyme-linked aptamer assay; EIS, electrical impedance spectroscopy; RNA, ribonucleic acid; ssDNA, single-stranded deoxyribonucleic acid.

Detection method	Aptamer	Selection against protein or virus	Specific target	K_D (binding affinity)	Selectivity	References
SPR	RNA	Whole HA	A/Panama/2007/1999 (H3N2)	188 pM	Cannot detect other H3N2 strains	[37]
SPR	RNA	Recombinant HA	HA of H5N1 and H7N7	170 pM	No cross reactivity with other subtypes	[43]
SPR	RNA	Whole HA	A/California/07/2009 (pandemic H1N1)	67 fM	Cannot detect other strains of H1N1 virus	[38]
SPR	RNA	Whole HA	Influenza B	720 pM	No cross reactivity with influenza A	[39]
SPR	DNA	Recombinant HA of H5N1 and H5N1 virus	H5N1 subtype	4.65 nM	No cross reactivity with other subtypes	[44]
ELAA	ssDNA	HA proteins	H1N1, H5N1, and H3N2	1.53×10^{-8} M	Specific to influenza A	[22]
ELAA	ssDNA	HA(91–261)	H1N1 (A/Puerto Rico/8/1934), H2N2 and H3N2		Not specific to H1N1 subtype alone	[23]
Fluorescent assay	ssDNA	Whole HA	H1N1 influenza A/Puerto Rico/8/1934	78 ± 1 nM	Cannot detect other strains of H1N1	[24]
ELAA, EIS aptasensor	ssDNA	Inactivated H1N1 virus	H1N1, H3N2, influenza B	5.54 ± 4.41 nM	Not specific to H1N1 subtype alone	[41]
Sandwich type SPR	ssDNA	Whole virus	H5Nx (H5N1, H5N8, H5N2)	8×10^4 to 1×10^4 EID50/mL	Specific to H5 subtype	[45]
Fluorescence assay, Voltammetry aptasensor	ssDNA	Mini HA 4900 and H1N1 virus	H1N1 subtype	19.2 nM	No cross reactivity with other subtypes	Present study

high-fidelity PCR master mix (New England BioLabs, Ipswich, MA, USA) according to the manufacturer's instructions and cloned into a pCDNA3.1 vector by restriction digestion and ligation. His-tagged mini-HA protein was produced in HEK293T cells by transient transfection of the recombinant vector with Lipofectamine 2000 (Invitrogen, Carlsbad, CA, USA). The HEK293T cells were cultured in Dulbecco's Modified Eagle's Medium with high glucose, 10% fetal bovine serum, and 1 × penicillin/streptomycin solution (Gibco, Thermo Fisher Scientific, Waltham, MA, USA) and were incubated at 37 °C in a humidified 5% CO_2 incubator. The His-tagged mini-HA was purified with the MagneHis protein purification system (Promega, Madison, WI, USA), according to the manufacturer's protocols. The purity of the eluted mini-HA protein was estimated by 10% sodium dodecyl sulfate-polyacrylamide gel electrophoresis.

2.2. In vitro selection of aptamers

A DNA library that consisted of randomized 40-mer DNA sequences flanked by primer-binding sites and appropriate primers was purchased from Trilink Biotechnologies (San Diego, CA, USA). The DNA library was amplified by PCR with the Phusion high-fidelity PCR master mix with HF buffer according to the manufacturer's protocols for 25 cycles. The amplified products were purified with the GeNetBiotech PCR purification kit (GeNetBiotech, Seoul, Korea), converted to ssDNA by denaturation at 95 °C for 10 min, followed by immediate snap-freezing on ice. Selection of the aptamer was carried out initially by incubation of the mini-HA protein (2 μg) with the amplified ssDNA library (10 nM) in 450 μL of binding buffer (MagneHis Protein Purification System) for 1 h with shaking at room temperature (RT). A volume of 5 μL of MagneHis Ni particles was added, incubated for 15 min, and washed with a washing buffer three times to remove unbound DNA. The bound ssDNA–mini-HA complexes were eluted with 50 μL of elution buffer (MagneHis Protein Purification System) and recovered by precipitation with 2.5 μL of 200 mM glycogen, 20 μL of 7.5 M sodium acetate, and 200 μL of 100% ethanol. The recovered complexes were re-suspended in 25 μL of nuclease-free water and used as the template in the next round of SELEX amplification and purification. After the execution of five rounds of SELEX with amplification followed by mini-HA selection, six rounds of SELEX were performed with H1N1 viruses. First, 400 plaque-forming units (PFU) of H1N1 (KBPV–VR–33) virus were included. The aptamers bound to the H1N1 virus were recovered by centrifugation for 1 h at 12,000 rpm and 4 °C. The supernatant was discarded, pelleted complexes were washed twice, and the aptamers were recovered by heating them at 95 °C for 5 min and collected by centrifugation at 12,000 rpm and 4 °C for use in the subsequent rounds of amplification and purification. Selection concentrations were gradually reduced over the SELEX process, from 2 μg to 125 ng for mini-HA protein and from 40 μL to 5 μL for H1N1 virus (10^4 PFU mL^{-1}), to obtain high-binding affinity aptamers (Table 2).

2.3. Enzyme-linked aptamer assay (ELAA)

ELAA was performed for the comparison of binding of the PCR products with mini-HA for 1–5 rounds and with H1N1 viruses for 6–11 rounds. The ssDNA pools from each round of selection were stored and amplified with biotinylated forward and reverse primers. A 96-well microtiter plate (Nunc, Roskilde, Denmark) was treated with either 250 ng of mini-HA protein or 40 μL of H1N1 virus (KBPV–VR–33) (10^4 PFU mL^{-1}) per well in 100 μL of carbonate buffer (pH 9.6) at 4 °C overnight. The plate was rinsed with phosphate buffered saline (PBS) and treated with super-block TBS buffer (Thermo Scientific) for 1 h at RT to preclude nonspecific binding. The biotinylated PCR products were diluted in PBS to a final concentration of 500 nM and denatured at 95 °C for 5 min. These ssDNA pools were added to the mini-HA protein- (1–5 rounds) or virus-coated wells (6–11 rounds), incubated for 1 h at RT, and washed with PBS three times. A volume of 50 μL of streptavidin–horseradish peroxidase (Abcam, Cambridge, UK) was added, and the mixture was incubated at RT for 30 min. The plate was washed again, 100 μL of 3,3′,5,5′-tetramethylbenzidine substrate solution (Sigma–Aldrich, St Louis, MO, USA) was added, and the plate was incubated for 10 min at RT. Sulfuric acid (0.5 N) was then added, and the absorbance (450 nm) was measured with a microplate reader.

Table 2
Concentrations of aptamers, targets, and incubation time for each cycle of systematic evolution of ligands by exponential enrichment (SELEX).

Cycle	HA protein (μg)	ssDNA Pool (nmole)	Incubation time (min)
1	2	10	60
2	1	10	60
3	0.5	7	45
4	0.25	7	45
5	0.125	7	30
	Virus (μL)		
6	40	7	30
7	30	5	30
8	20	4	25
9	10	3	25
10	5	2	20
11	5	2	20

2.4. Cloning and sequencing of aptamer candidates

The aptamer pools at the final round were amplified and purified as described above. The purified DNA products were cloned using the pGEM-T Easy Vector system (Promega) and transformed into chemically competent TOP10 *Escherichia coli* cells (Invitrogen) by heat shock at 42 °C. The transformed cells were plated on Luria–Bertani (LB) agar with ampicillin (50 μg mL^{-1}), and 60 randomly selected bacterial colonies were picked and grown in LB broth (6 mL) containing ampicillin (50 μg mL^{-1}) at 37 °C overnight by shaking at 150 rpm. Plasmids were isolated with the PureYield Plasmid Miniprep system (Promega) and sequenced by Macrogen (Seoul, South Korea). The sequences of selected aptamers were further processed for secondary structure prediction with the software NUPACK [25] and FOLD [26].

2.5. Quantification of target-bound aptamers using qPCR

All qPCR amplification and analyses were performed with a LightCycler 480 II instrument. A PCR reaction mixture (20 μL) was prepared with 10 μL of Power SYBR Green PCR Master mix (Applied Biosystems, Foster City, CA, USA), 2 μL of primer pair mix (5 pmol μL^{-1} each primer), 3 μL of DNA template, and 5 μL of nuclease-free water. The ssDNA aptamers at both the 10th and 11th rounds were incubated with the mini-HA protein (250 ng) rather than the influenza virus H1N1, owing to the safety of the process, in binding buffer at a final volume of 50 μL for 2 h. Target-bound aptamers were pulled down and eluted as described above, and 5-μL aliquots were then used as a qPCR template for all the aptamers. The amplification cycle was completed as follows: an initial denaturation at 95 °C for 10 min, followed by 40 cycles (10 s at 95 °C, 10 s at 60 °C, and 10 s at 72 °C) with fluorescence signal measurements after each extension step. All qPCR measurements were performed in duplicate. A standard curve was determined using aliquots of a 10-fold serial dilution of the random

ssDNA library as qPCR templates, to enable the extrapolation of the copy numbers of target-bound aptamers. Background measurements were subtracted for each sample. The dissociation constant (K_D) was calculated by nonlinear fitting to $Y = B_{max} \times X/(K_D + X)$, where Y is the normalized signal, X is the concentration of the aptamer (nM), and B_{max} is the maximum signal.

2.6. Fluorescence affinity measurement

Different concentrations of carboxyfluorescein (FAM)-labeled ssDNA aptamers V46 and V57 were incubated for 2 h with mini-HA protein (250 ng) in binding buffer (MagneHis Protein Purification System) at RT, followed by the addition of 5 μL of Magne-His Ni particles (MagneHis Protein Purification System). The aptamers were incubated for 15 min, washed three times with binding buffer (MagneHis Protein Purification System), and the bound aptamers were eluted with elution buffer (50 μL) (MagneHis Protein Purification system). The eluted aptamers were calculated by fluorescence intensity measurements with a microplate reader (excitation wavelength 490 nm, and emission wavelength 520 nm), and K_D was calculated by nonlinear regression fitting as described above.

2.7. Voltammetry measurement of the binding affinity

Chemically modified indium tin oxide (ITO)/glass electrodes were used for binding affinity measurements using voltammetry. An immobilization scheme on the ITO/glass electrodes is given in supplementary information (Fig. S1). Cyclic voltammetry (CV) were performed to characterize the modified ITO/glass electrodes after each modification step over the potential range (−0.65 V to + 0.5 V) with a scan rate of 50 mV s^{-1}. Binding assays were performed with various aptamer concentrations (0–250 nM) and 250 nM of random sequence 5′-TTCGACCGCGGTTATAAGACTCAT-3' (Macrogen) as a negative control (NTC) using differential pulse voltammetry (DPV). DPV was also performed at a potential range (−0.8 V to +0.8 V) with a pulse amplitude of 50 mV and a scan rate of 100 mVs^{-1}. The CV and DPV measurements were performed in the presence of 1 × PBS (pH 7) solution containing 5 mM $[Fe(CN)_6]^{3-/4-}$ and 0.5 M KCl as the redox probe. The Langmuir isotherm (nonlinear regression fitting) was used for K_D determination, based on the formula $\Delta I = (\Delta I)_{max}\,[C/K_D + C]$, where ΔI is the change in current ($I_{0\ (blank)} - I_{(test\ samples)}$), and C is the aptamer concentration.

2.8. Fabrication of an aptasensor using the developed aptamer

An ITO coated glass wafer was diced into electrode strips (2 cm × 0.5 cm), and the strips were cleaned in acetone, methanol, and DI water sequentially. The ITO/glass strips were ultrasonically cleaned using acetone, soap solution, and distilled water for 5 min each and was dried under a stream of N_2 gas. These strips were immersed in a solution containing NH_4OH, H_2O_2, and H_2O, at a volume ratio of 1:1:5 for 30 min at 60 °C to form hydroxyl groups on the surface of the ITO. The modified strips were washed with distilled water and dried gently with N_2 gas. A working area of 0.1 cm^2 was used for further modification and the remaining area was covered with tapes to prevent the deposition. Positive charges were introduced by immersing the working areas of the ITO/glass strips in 1% polyethylenimine (PEI) solution for 2 h followed by incubation with the negatively charged V46 aptamer (100 nM), which corresponded to 3.9×10^{13} molecules/cm^2. Physically adsorbed aptamers were removed by immersion in ultrapure water. Finally, the V46–PEI–ITO electrode was immersed in 1% BSA solution to block active sites.

2.9. Electrochemical measurements

Cyclic voltammetry (CV) and electrochemical impedance spectroscopy (EIS) were performed to characterize the modified ITO electrodes (aptasensors). The CV was recorded from −0.8 V to +0.8 V with a scan rate of 50 mVs^{-1}. The impedance measurements were performed in the frequency range of 0.1 Hz–100 kHz and an amplitude of 10 mV. For detection of the H1N1 virus, 10-μL droplets containing various virus concentrations (KBPV–VR–33) (10^0 to 10^6 PFU mL^{-1}) were incubated on the aptamer-modified electrodes for 30 min and washed with PBS to remove unbound viruses, followed by DPV measurements. Selectivity experiments of the aptasensors were performed by incubating them with six strains of H1N1 influenza A viruses [KBPV–VR–33, KBPV–VR–76, ATCC–VR–98 (A/Mal/302/54), ATCC–VR–97 (A/FM/1/47), ATCC–VR–219 (A/NWS/33), and ATCC–VR–1736 (A/Virginia/2009)], two strains of H3N2 influenza A viruses (KBPV–VR–71 and ATCC–VR–1837), adenovirus virus (KBPV–VR–4), and influenza B virus (IV–B; KBPV–VR–34), where all the virus concentrations were 10^6 PFU mL^{-1}, and 250 ng of HA proteins of four different subtypes of influenza A viruses: H5N1 (A/Anhui/1/2005), H1N2 (A/swine/Guangxi/13/2006), H1N3 (A/duck/NZL/160/1976), and H1N8 (A/Egyptian/South Africa/AI1448/2007/) (Sino Biological, Wayne, PA, USA). DPV was carried out over the potential range of −0.8 V to +0.8 V, with a pulse amplitude of 50 mV and a scan rate of 100 mVs^{-1} using an Autolab Potentiostat/Galvanostat (PGSTAT204, Metrohm, Barendrecht, Netherlands) in 1 × PBS solution that contained 5 mM $[Fe(CN)_6]^{3-/4-}$ and 0.5 M KCl as the redox probe.

2.10. Statistical analysis

All experiments were performed in triplicate. Error bars represent the standard deviation of three measurements.

3. Results and discussion

3.1. Selection of target-bound aptamers by SELEX

After five rounds of SELEX with the mini-HA protein and six rounds with the H1N1 virus (Fig. 1A), binding of ssDNAs from each round was assessed using ELAA. The level of binding of the ssDNA pool increased as the SELEX progressed from the first to the fifth round and from the sixth to the eleventh selection cycle (Fig. 1B). The selectivity was increased throughout the SELEX by decreasing the amounts of ssDNA and either the mini-HA protein or the H1N1 virus (Table 2) to promote specific binding between these targets and the selected aptamers. Binding of the ssDNA pool to the H1N1 virus did not differ significantly between the tenth and eleventh selection rounds, suggesting the maximum binding affinity towards the target. Therefore, the eluted ssDNA aptamer pools from the tenth and eleventh rounds of SELEX were PCR-amplified, cloned, and sequenced. Clones without aptamer sequences were excluded from further analyses. Several aptamer sequences were repeatedly found in two or more clones, indicating that these repeated sequences had a high binding affinity [27]. Complete sequencing results are shown in Table S1.

3.2. Evaluation and characterization of candidate aptamers

The level of binding was evaluated by incubating the aptamers with the mini-HA protein and quantifying the copy numbers of the bound aptamers with qPCR (Fig. 1C). A total of 11 ssDNA aptamers with high copy numbers or repeated sequences were selected for further evaluation (Table 3). The binding affinities of these selected aptamers were assessed by qPCR after incubation of different

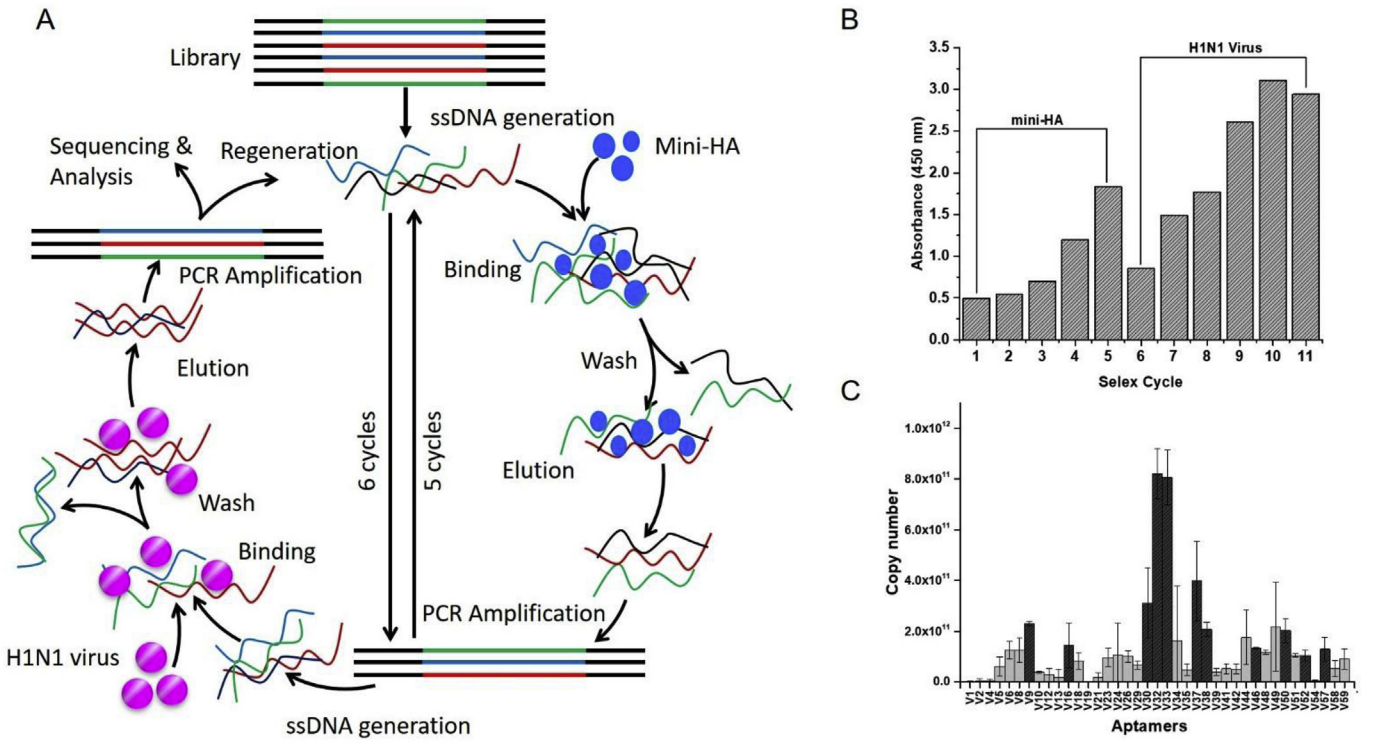

Fig. 1. Outline of the systematic evolution of ligands by exponential enrichment (SELEX) process. **(A)** A library consisting of randomized 40-mer ssDNA sequences was used for selection of aptamers via five rounds of SELEX with a recombinant influenza A mini-hemagglutinin (mini-HA) stem protein, and six rounds with influenza H1N1 whole viruses (KBPV–VR–33). The concentrations of the mini-HA protein and H1N1 viruses were gradually reduced in subsequent cycles to obtain high-binding-affinity aptamers. **(B)** Parallel binding measurements of PCR products from each round of SELEX were performed after amplification of ssDNA pools with biotinylated primers. **(C)** Selection of aptamers with a high level of binding from randomly selected clones based on qPCR analyses. Aptamers were incubated with mini-HA protein in 50 μL (final volume) of binding buffer for 2 h, unbound ssDNA was removed by washing, and the level of binding of each aptamer was measured by qPCR. Eleven aptamer sequences with high copy numbers or repeated sequences (dark colored bars) were selected for further analysis.

Table 3
Binding affinity (K_D) determined by qPCR and the corresponding sequences of the 11 selected aptamers. Aptamers with data that did not fit the equilibrium binding curves were excluded from further analysis, and their dissociation constants are indicated as not being available (N/A).

Aptamers	Sequence	K_D
V9	GACGTGGTGACGGTGGGGTGGAACGTGCCGTGTGCGTGGT	N/A
V16	TCGTTGGGCTGGGCTGCGATGGTTGGTGAGACTCGGCGTG	N/A
V30	GCCACGTACGCCTCATCGCCCACCCTCACTGCACCTCGCC	99.8 ± 24.9
V32	CGCGAGAGCAGCTGGGGGGAGGGCGTGGCAGGTGGTGTGG	N/A
V33	CACGGACGGACGGCACAGTGGAGGGAGGCACACCGCGGTG	N/A
V37	CCACCTCACAACGACACCACAACCCCGTACGCCACATCGG	835.8 ± 159.2
V38	GGACACGTGCGGACTGTGGTCATGTGACGCATGGTGCAGG	118.4 ± 36.8
V46	TACTGCACACGACACCGACTGTCACCATCACCTCGGCGCA	20.7 ± 3.8
V50	GGACACAGAGGGCAAGATGTGTGTAGGATGGGTAGGGTCA	NA
V52	AGCACAGAGTTGGAAACATGACCCCGACCCGCCGCGTTGA	311.5 ± 151.9
V57	CGCAACACACCATCCCCCTTGCATTCCGCACACCACGCTT	66.7 ± 18.3

concentrations of the aptamers with the mini-HA protein (250 ng) and removal of unbound aptamers. The qPCR results enabled the calculation of the K_D values for each of these aptamers by nonlinear fitting, and the K_D values ranged from 20.7 nM to 835.8 nM (Table 3). Aptamers V46 and V57 yielded the highest affinities, with K_D values of 20.7 ± 3.8 nM and 66.7 ± 18.3 nM, respectively. These two aptamers demonstrated sufficient affinities considering that K_D values for many antibodies range between 1 nM and 100 nM [28,29], and their binding affinities were further evaluated by fluorescence measurements (Fig. 2A). Different concentrations of FAM-labeled V46 and V57 aptamers were incubated with the mini-HA (250 ng), and the fluorescence intensities of eluted bound aptamers were measured to calculate the K_D values using the Langmuir binding isotherm [30,31], eliciting values of 29.1 ± 6.2 nM for V46 and 36.1 ± 16.0 nM for V57. These results indicated that V46 had a higher binding affinity than V57 to the mini-HA protein.

The secondary structures of the aptamer sequences, as determined with the Fold web server, showed the presence of CACC (also in 5′ and 3’ complementary sequences captured with forward and reverse primers) in the loops of the majority of aptamer sequences (Fig. 2B, Fig. S2). It has been reported that the secondary loops and repeating sequences of C nucleotides are important to producing high affinity aptamers for viruses [32]. Interestingly, aptamer V46 contained three CACC (highlighted in red) in the stem and loop motif altogether (Fig. 2B, Table 3).

3.3. K_D determination using an electrochemical assay

To further evaluate aptamers V46 and V57, mini-HA immobilized ITO electrodes were developed (Fig. S1) and electroanalytical

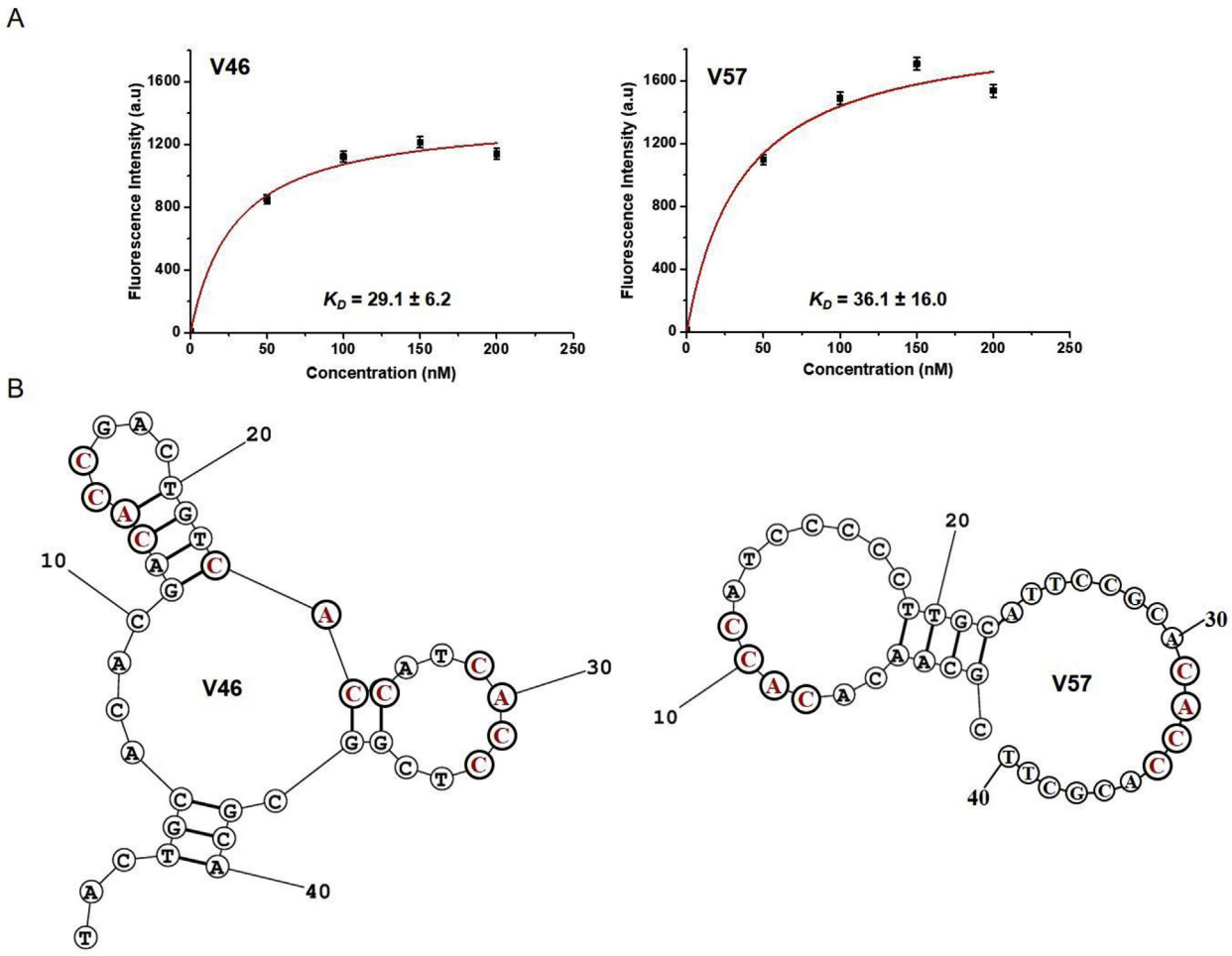

Fig. 2. Binding affinity measurements and secondary structure prediction of two selected aptamers, V46 and V57. These two aptamers were incubated with a fixed amount of recombinant influenza A mini-hemagglutinin (mini-HA) stem protein, unbound aptamers were removed by washing, and the levels of bound aptamers were measured by fluorescence. **(A)** Equilibrium binding curves of V46 and V57 aptamers analyzed by fluorescence assays. **(B)** The secondary structure of V46 and V57 aptamers was determined using the RNA fold software. The predicted secondary structure shows two stem loops with three CACC motifs (in red) in aptamer V46 and one stem loop with one CACC sequence in aptamer V57. (For interpretation of the references to color in this figure legend, the reader is referred to the Web version of this article.)

measurements were acquired using negative control (NTC) and various concentrations of the aptamers. The peak current changed after each successive modification of the ITO with APTES, GA, mini-HA, and BSA (Fig. 3A). Differences in peak current ($\Delta I = I_o - I$) with the final mini-HA immobilized electrode were observed before and after the binding of the aptamers (Fig. 3B, insets). The change in peak current owing to NTC attachment was negligible (relative change < 2%), indicating the low probability of false positive results. The peak currents showed concentration-dependent decreases with the addition of the aptamers because of the repulsion of the redox probe by the negatively charged DNA on the modified electrode, which obstructed the transfer of electrons. Based on this method, the K_D values were determined as 19.2 ± 5.7 nM for V46 and 29.6 ± 8.8 nM for V57 (Fig. 3B).

The predicted secondary structure of aptamer V46 showed two stem loops (CACC motif), which may not only facilitate high binding affinity and specificity but also enable stable binding interaction with H1N1 influenza A viruses and mini-HA proteins compared to aptamer V57, which contains only one stable stem loop. The CACC motif was also present in the stem-loop sequence of a high binding affinity RNA aptamer (D-26) [33]; however, this aptamer failed to bind with HA proteins of different strains of H1N1, demonstrating its strain-specificity. Moreover, RNA aptamers are not stable in comparison to DNA aptamers [34–36]. Therefore, aptamer V46 was further evaluated by DPV measurements to assure the stable binding interaction with different strains of the H1N1 virus, where the viruses were immobilized on the same ITO electrodes instead of mini-HA (Fig. S1). The estimated K_D values for V46 against the KBPV–VR–33, KBPV–VR–76, ATCC–VR–97, ATCC–VR–98, ATCC–VR–219, and ATCC–VR–1736 strains of H1N1 virus were 25.1 ± 10.0 nM, 33.5 ± 13.8 nM, 57.1 ± 15.9 nM, 12.5 ± 7.3 nM, 14.3 ± 6.5 nM, and 8.2 ± 1.1 nM, respectively (Fig. 4). Although several RNA [37–39] and DNA [22–24,40] aptamers have been reported for influenza A viruses, this is the first report of the selection of ssDNA aptamers targeting the mini-HA to enable the detection of a broad range of H1N1 virus strains. This report contrasts with the DNA aptamers previously developed using HA proteins [22–24,40].

3.4. Electrochemical aptasensor for H1N1 virus

The results described above indicate that aptamer V46 can be used for electrochemical subtyping of H1N1 virus; therefore, the aptamer was incorporated into a label-free biosensor platform for the influenza A H1N1 virus. CV and EIS measurements were performed for the characterization of the aptamer-modified ITO

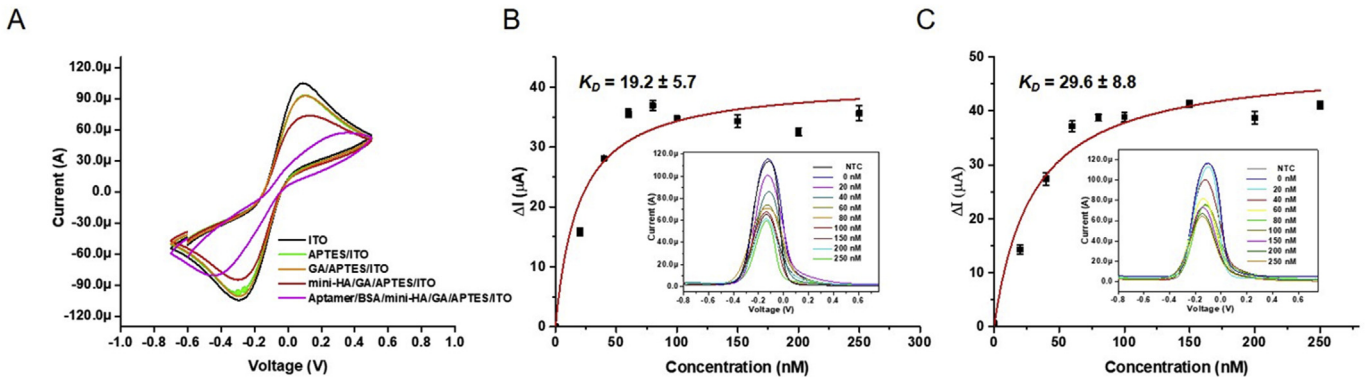

Fig. 3. **(A)** Cyclic voltammograms of ITO, (3-aminopropyl)trimethoxysilane (APTES)–ITO, glutaraldehyde (GA)–APTES–ITO, mini-HA–GA–APTES–ITO, and bovine serum albumin (BSA)–mini-HA–GA–APTES–ITO. **(B)** Differential pulse voltammetry analyses of the binding affinity between mini-HA and various concentrations (0–300 nM) of aptamers V46 and V57 in the presence of 1 × phosphate buffered saline (PBS) solution containing 5 mM $[Fe(CN)_6]^{3-/4-}$ and 0.5 M KCl as a redox probe.

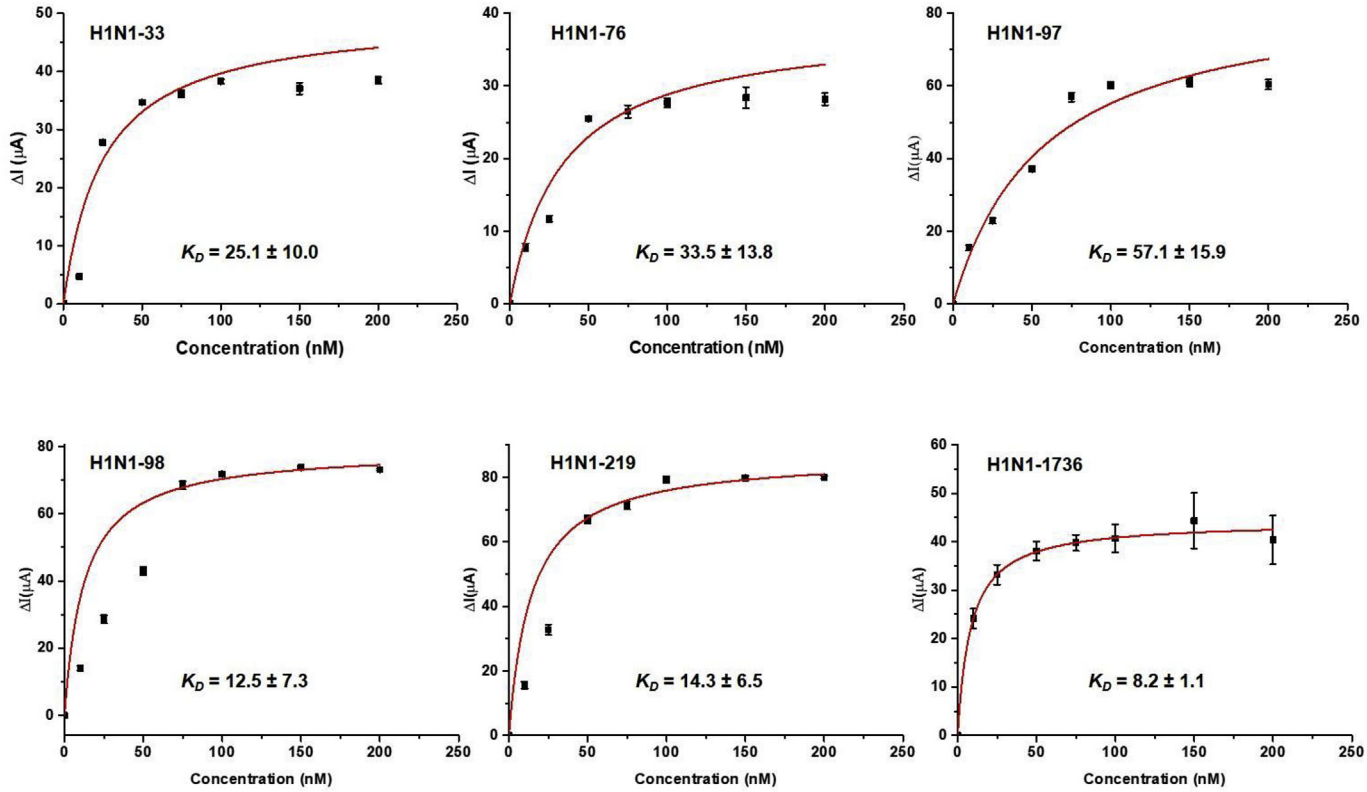

Fig. 4. Binding affinity (K_D) of aptamer V46 determined using differential pulse voltammetry for various strains of the influenza H1N1 virus (KBPV-VR-33, KBPV-VR-76, ATCC-VR-97, ATCC-VR-98, ATCC-VR-219, and ATCC-VR-1736) and various concentrations (0–200 nM) of aptamer V46 in the presence of 1 × phosphate buffered saline (PBS) containing 5 mM $[Fe(CN)_6]^{3-/4-}$ and 0.5 M KCl as a redox probe.

electrodes (aptasensor) (Fig. 5A). The amount of current for a PEI–ITO electrode (peak current, 298 μA) was higher than that for a bare ITO electrode (peak current, 267 μA), which demonstrated the conductive nature of PEI (Fig. 5B). The peak current decreased to 51.3 μA after the aptamer was immobilized. BSA was then used for preventing nonspecific binding on the V46–PEI–ITO electrode, leading to a further decrease in the peak current (49.2 μA). The modification of the ITO electrode was also confirmed by impedance measurements (Fig. 5C). The straight line response of the PEI–ITO electrode in comparison to the small semicircle (Rct = 71Ω) for the ITO electrode indicates the rapid electron-transfer kinetics associated with the conducting PEI layer on the ITO electrode. However, after the aptamer was added onto the electrodes, the charge transfer resistance was increased owing to the repulsion of ferri/ferro ions by the anionic ssDNA aptamer. The resistance was further increased upon addition of BSA. These impedance results were in good agreement with the CV measurements, thus indicating the successful modification of the ITO electrode.

To determine the measurement range of the aptasensor, voltammetric responses were monitored for various concentrations of H1N1 (KBPV–VR–33) that ranged from 1 to 10^6 PFU mL^{-1}. The peak current decreased with increasing H1N1 virus concentration (Fig. 5D, inset). The graph shows a linear relationship from 10^1 PFU mL^{-1} to 10^4 PFU mL^{-1}, and the regression equation is I_p

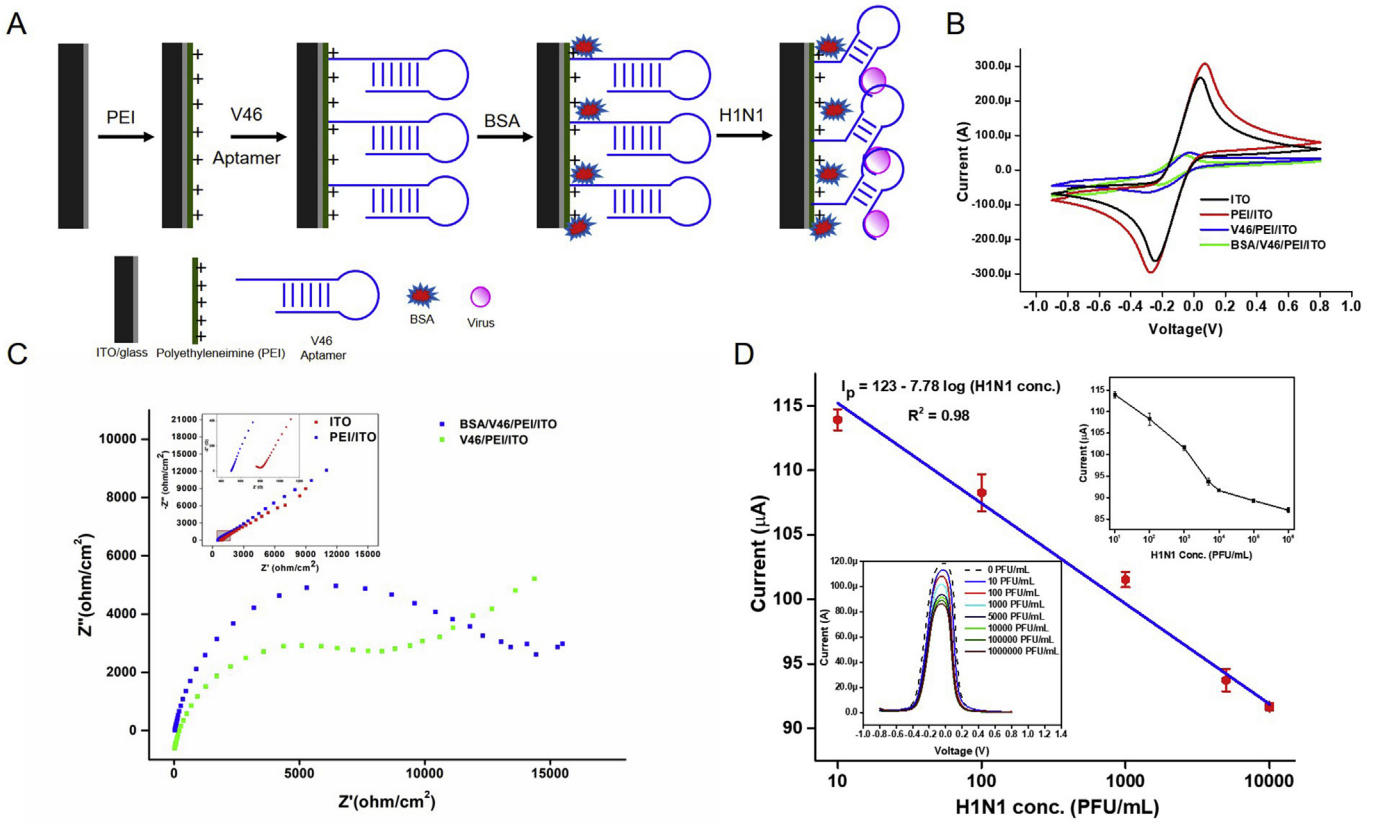

Fig. 5. Fabrication and testing of an aptamer-based H1N1 sensor (aptasensor). **(A)** Fabrication process of an aptasensor using aptamer V46. **(B)** Cyclic voltammograms of indium tin oxide (ITO), polyethylenimine (PEI)–ITO, V46–PEI–ITO, and bovine serum albumin (BSA)–V46–PEI–ITO. **(C)** Electrochemical impedance spectroscopic analysis of ITO, PEI–ITO (inset), V46–PEI–ITO, and BSA–V46–PEI–ITO. **(D)** Linear calibration graph showing the change in peak current at various concentrations of H1N1 (10^1–10^4 plaque-forming units mL^{-1}). Differential pulse voltammograms with a wider range of concentrations of H1N1 viruses are shown in the inset.

(μA) = 123−7.78 log C [PFU mL^{-1}] ($R^2 = 0.98$). The limit of detection (LOD) of the V46 aptasensor for H1N1 was 3.7 PFU mL^{-1} based on three standard deviations of the blank signal in the linear portion of the calibration curve. Bai et al. [41] also developed a highly sensitive electrochemical aptasensor for detection of H1N1 viruses with LOD of 0.9 pg μL^{-1}. However, this aptasensor was not only specific to H1N1 subtypes, but was also specific to H1N3 as well as influenza B virus, because the binding affinity of the aptamer used in this work

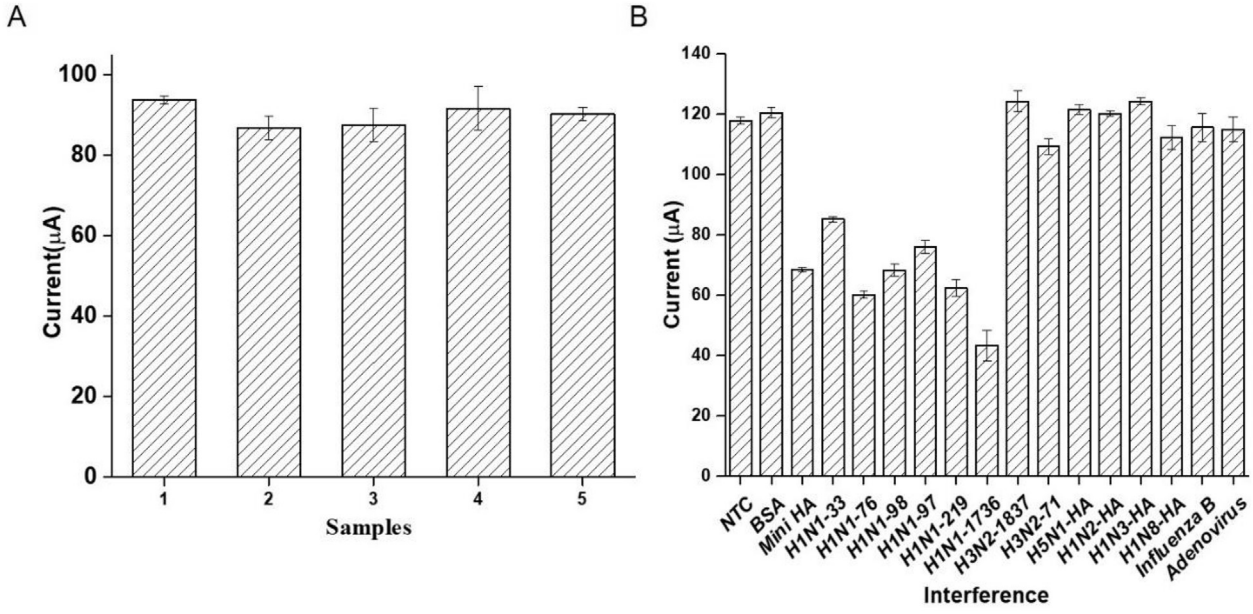

Fig. 6. **(A)** Reproducibility of aptasensors **(B)** Qualitative specificity analyses of aptamer V46 against several strains of H1N1 subtype, other subtypes, and other viruses using differential pulse voltammetry. All the virus concentrations were 10^6 PFU mL^{-1}.

was based on probe density; therefore, it is not appropriate for subtyping.

3.5. Reproducibility and selectivity

To evaluate the reproducibility of the immunosensors, a series of five different devices were prepared for the detection of 10^4 PFU mL^{-1} of H1N1 virus (Fig. 6A). The relative standard deviation (RSD) of the measurements for the five devices was 5.95%, indicating that the reproducibility of the immunosensors was acceptable. In the present study, the selectivity of the aptasensor was tested with various stains of H1N1 viruses and other subtypes of the influenza virus using DPV (Fig. 6B). The decreases in current compared to the NTC case were large for the mini-HA and 6 strains of H1N1 viruses but were very small for other subtypes (H3N2, H5N1, H1N2, H1N3, and H1N8), adenovirus, and influenza B virus. These results suggest that this V46 aptamer-based electrochemical sensor had high binding affinity and high specificity to a broad range of H1N1 strains compared to other influenza sensors and clinically observed virus concentrations [42]; therefore, this technology can be used for electrochemical subtyping of H1N1 virus along with its quantification.

4. Conclusion

We presented ssDNA aptamers with high affinity and high specificity to influenza A H1N1 viruses based on the mini-HA (recombinant, stable and conserved stem region) and whole H1N1 viruses via SELEX. The K_D value of aptamer V46 was obtained as 19.2 nM according to the DPV analysis. We also developed a label-free electrochemical aptasensor using the aptamer for rapid subtyping of influenza A H1N1 virus. This is the first study on the development of a DNA aptamer for rapid subtyping of influenza A H1N1 virus. This DNA aptasensor-based subtyping is low-cost, easy to perform, and quicker than the standard ELISA and nucleic acid-based methods and has the potential to be used in clinical laboratories.

Conflicts of interest

The authors have no conflicts to declare.

Acknowledgments

This research was supported by the MSIT (Ministry of Science and ICT), Korea, under the ITRC support program (IITP-2018-2017-0-01635) supervised by the IITP, and the 2018 Research Fund (1.180015.01) of UNIST.

Appendix A. Supplementary data

Supplementary data to this article can be found online at https://doi.org/10.1016/j.aca.2019.03.005.

References

[1] M. Wongphatcharachai, P. Wang, S. Enomoto, R.J. Webby, M.R. Gramer, A. Amonsin, S. Sreevatsan, Neutralizing DNA aptamers against swine influenza H3N2 viruses, J. Clin. Microbiol. 51 (2013) 46–54, https://doi.org/10.1128/JCM.02118-12.

[2] Y. Peng, D. Wang, J. Wang, K. Li, Z. Tan, Y. Shu, T. Jiang, A universal computational model for predicting antigenic variants of influenza A virus based on conserved antigenic structures, Sci. Rep. 7 (2017), https://doi.org/10.1038/srep42051.

[3] C.-Y. Wu, C.-W. Lin, T.-I. Tsai, C.-C.D. Lee, H.-Y. Chuang, J.-B. Chen, M.-H. Tsai, B.-R. Chen, P.-W. Lo, C.-P. Liu, V.S. Shivatare, C.-H. Wong, Influenza A surface glycosylation and vaccine design, Proc. Natl. Acad. Sci. Unit. States Am. 114 (2017) 280–285, https://doi.org/10.1073/pnas.1617174114.

[4] S.A. Valkenburg, V.V.A. Mallajosyula, O.T.W. Li, A.W.H. Chin, G. Carnell, N. Temperton, R. Varadarajan, L.L.M. Poon, Stalking influenza by vaccination with pre-fusion headless HA mini-stem, Sci. Rep. 6 (2016) 22666, https://doi.org/10.1038/srep22666.

[5] M.G. Joyce, A.K. Wheatley, P.V. Thomas, G.-Y. Chuang, C. Soto, R.T. Bailer, A. Druz, I.S. Georgiev, R.A. Gillespie, M. Kanekiyo, W.-P. Kong, K. Leung, S.N. Narpala, M.S. Prabhakaran, E.S. Yang, B. Zhang, Y. Zhang, M. Asokan, J.C. Boyington, T. Bylund, S. Darko, C.R. Lees, A. Ransier, C.-H. Shen, L. Wang, J.R. Whittle, X. Wu, H.M. Yassine, C. Santos, Y. Matsuoka, Y. Tsybovsky, U. Baxa, J.C. Mullikin, K. Subbarao, D.C. Douek, B.S. Graham, R.A. Koup, J.E. Ledgerwood, M. Roederer, L. Shapiro, P.D. Kwong, J.R. Mascola, A.B. McDermott, Vaccine-induced antibodies that neutralize group 1 and group 2 influenza a viruses, Cell 166 (2016) 609–623, https://doi.org/10.1016/j.cell.2016.06.043.

[6] K.L. Kaul, K.A. Mangold, H. Du, K.M. Pesavento, J. Nawrocki, J.A. Nowak, Influenza a subtyping: seasonal H1N1, H3N2, and the appearance of novel H1N1, J. Mol. Diagnostics. 12 (2010) 664–669, https://doi.org/10.2353/JMOLDX.2010.090225.

[7] J. Johnson, A. Higgins, A. Navarro, Y. Huang, F.L. Esper, N. Barton, D. Esch, C. Shaw, P.D. Olivo, L.Y. Miao, Subtyping influenza A virus with monoclonal antibodies and an indirect immunofluorescence assay, J. Clin. Microbiol. 50 (2012) 396–400, https://doi.org/10.1128/JCM.01237-11.

[8] T. Ziegler, H. Hall, A. Sánchez-Fauquier, W.C. Gamble, N.J. Cox, Type- and subtype-specific detection of influenza viruses in clinical specimens by rapid culture assay, J. Clin. Microbiol. 33 (1995) 318–321. http://www.ncbi.nlm.nih.gov/pubmed/7714186. (Accessed 10 October 2018).

[9] World Health Organization, WHO Guidelines for Pharmacological Management of Pandemic Influenza (H1N1) 2009 and Other Influenza Viruses Part I: Recommendations, 2009.

[10] K. Groff, J. Brown, A.J. Clippinger, Modern affinity reagents: recombinant antibodies and aptamers, Biotechnol. Adv. 33 (2015) 1787–1798, https://doi.org/10.1016/j.biotechadv.2015.10.004.

[11] K. Houser, K. Subbarao, Influenza vaccines: challenges and solutions, Cell Host Microbe 17 (2015) 295–300, https://doi.org/10.1016/j.chom.2015.02.012.

[12] P. Chames, M. Van Regenmortel, E. Weiss, D. Baty, Therapeutic antibodies: successes, limitations and hopes for the future, Br. J. Pharmacol. 157 (2009) 220–233, https://doi.org/10.1111/j.1476-5381.2009.00190.x.

[13] J.-W. Park, R. Tatavarty, D.W. Kim, H.-T. Jung, M.B. Gu, Immobilization-free screening of aptamers assisted by graphene oxide, Chem. Commun. 48 (2012) 2071–2073, https://doi.org/10.1039/C2CC16473F.

[14] A.D. Keefe, S. Pai, A. Ellington, Aptamers as therapeutics, Nat. Rev. Drug Discov. 9 (2010) 537–550, https://doi.org/10.1038/nrd3141.

[15] T. Šmuc, I.Y. Ahn, H. Ulrich, Nucleic acid aptamers as high affinity ligands in biotechnology and biosensorics, J. Pharm. Biomed. Anal. 81–82 (2013) 210–217, https://doi.org/10.1016/j.jpba.2013.03.014.

[16] S.D. Jayasena, Aptamers: an emerging class of molecules that rival antibodies in diagnostics, Clin. Chem. 45 (1999). http://clinchem.aaccjnls.org/content/45/9/1628.long. (Accessed 18 August 2017).

[17] J.J. Skehel, D.C. Wiley, Receptor binding and membrane fusion in virus entry: the influenza hemagglutinin, Annu. Rev. Biochem. 69 (2000) 531–569, https://doi.org/10.1146/annurev.biochem.69.1.531.

[18] R.J. Russell, D.J. Stevens, L.F. Haire, S.J. Gamblin, J.J. Skehel, Avian and human receptor binding by hemagglutinins of influenza A viruses, Glycoconj. J. 23 (2006) 85–92, https://doi.org/10.1007/s10719-006-5440-1.

[19] X. Xiong, S.R. Martin, L.F. Haire, S. a Wharton, R.S. Daniels, M.S. Bennett, J.W. McCauley, P.J. Collins, P. a Walker, J.J. Skehel, S.J. Gamblin, Receptor binding by an H7N9 influenza virus from humans, Nature 499 (2013) 496–499, https://doi.org/10.1038/nature12372.

[20] A. Impagliazzo, F. Milder, H. Kuipers, M. Wagner, X. Zhu, R.M.B. Hoffman, R. van Meersbergen, J. Huizingh, P. Wanningen, J. Verspuij, M. de Man, Z. Ding, A. Apetri, B. Kükrer, E. Sneekes-Vriese, D. Tomkiewicz, N.S. Laursen, P.S. Lee, A. Zakrzewska, L. Dekking, J. Tolboom, L. Tettero, S. van Meerten, W. Yu, W. Koudstaal, J. Goudsmit, A.B. Ward, W. Meijberg, I.A. Wilson, K. Radošević, A stable trimeric influenza hemagglutinin stem as a broadly protective immunogen, Science 349 (6254) (2015) 1301–1306.

[21] H.-M. Woo, J.-M. Lee, S. Yim, Y.-J. Jeong, Isolation of single-stranded DNA aptamers that distinguish influenza virus hemagglutinin subtype H1 from H5, PLoS One 10 (2015), https://doi.org/10.1371/journal.pone.0125060 e0125060.

[22] I. Shiratori, J. Akitomi, D.A. Boltz, K. Horii, M. Furuichi, I. Waga, Selection of DNA Aptamers that Bind to Influenza A Viruses with High Affinity and Broad Subtype Specificity, 2014, https://doi.org/10.1016/j.bbrc.2013.11.041.

[23] S.H. Jeon, B. Kayhan, T. Ben-Yedidia, R. Arnon, A DNA aptamer prevents influenza infection by blocking the receptor binding region of the viral hemagglutinin, J. Biol. Chem. 279 (2004) 48410–48419, https://doi.org/10.1074/jbc.M409059200.

[24] W. Li, X. Feng, X. Yan, K. Liu, L. Deng, A DNA aptamer against influenza a virus: an effective inhibitor to the hemagglutinin–glycan interactions, Nucleic Acid Therapeut. 26 (2016) 166–172, https://doi.org/10.1089/nat.2015.0564.

[25] J.N. Zadeh, C.D. Steenberg, J.S. Bois, B.R. Wolfe, M.B. Pierce, A.R. Khan, R.M. Dirks, N.A. Pierce, NUPACK: analysis and design of nucleic acid systems, J. Comput. Chem. 32 (2011) 170–173, https://doi.org/10.1002/jcc.21596.

[26] D.H. Mathews, M.D. Disney, J.L. Childs, S.J. Schroeder, M. Zuker, D.H. Turner, Incorporating chemical modification constraints into a dynamic programming algorithm for prediction of RNA secondary structure, Proc. Natl. Acad. Sci. U.S.A. 101 (2004) 7287–7292, https://doi.org/10.1073/pnas.0401799101.

[27] M. Cho, Y. Xiao, J. Nie, R. Stewart, A.T. Csordas, S.S. Oh, J.A. Thomson, H.T. Soh, Quantitative selection of DNA aptamers through microfluidic selection and high-throughput sequencing, Proc. Natl. Acad. Sci. Unit. States Am. 107 (2010) 15373–15378, https://doi.org/10.1073/pnas.1009331107.
[28] P.S. Lee, R. Yoshida, D.C. Ekiert, N. Sakai, Y. Suzuki, A. Takada, I.A. Wilson, Heterosubtypic Antibody Recognition of the Influenza Virus Hemagglutinin Receptor Binding Site Enhanced by Avidity, (n.d.). doi:10.1073/pnas.1212371109.
[29] M. Hong, P.S. Lee, R.M.B. Hoffman, X. Zhu, J.C. Krause, N.S. Laursen, S.-I. Yoon, L. Song, L. Tussey, J.E. Crowe, A.B. Ward, I.A. Wilson, Antibody Recognition of the Pandemic H1N1 Influenza Virus Hemagglutinin Receptor Binding Site, (n.d.). doi:10.1128/JVI.01388-13.
[30] M. Cho, S. Soo Oh, J. Nie, R. Stewart, M. Eisenstein, J. Chambers, J.D. Marth, F. Walker, J.A. Thomson, H.T. Soh, Quantitative selection and parallel characterization of aptamers, Proc. Natl. Acad. Sci. U.S.A. 110 (2013), https://doi.org/10.1073/pnas.1315866110, 18460–5.
[31] G. Kemmer, S. Keller, Nonlinear least-squares data fitting in Excel spreadsheets, Nat. Protoc. 5 (2010) 267–281, https://doi.org/10.1038/nprot.2009.182.
[32] B. Musafia, R. Oren-Banaroya, S. Noiman, Designing anti-influenza aptamers: novel quantitative structure activity relationship approach gives insights into aptamer – virus interaction, PLoS One 9 (2014), e97696, https://doi.org/10.1371/journal.pone.0097696.
[33] S.C.B. Gopinath, P.K.R. Kumar, Aptamers that bind to the hemagglutinin of the recent pandemic influenza virus H1N1 and efficiently inhibit agglutination, Acta Biomater. 9 (2013) 8932–8941, https://doi.org/10.1016/j.actbio.2013.06.016.
[34] Q. Zhu, G. Liu, M. Kai, DNA aptamers in the diagnosis and treatment of human diseases, Molecules 20 (2015) 20979–20997, https://doi.org/10.3390/molecules201219739.
[35] Y.-T. Lai, J.J. DeStefano, DNA aptamers to human immunodeficiency virus reverse transcriptase selected by a primer-free SELEX method: characterization and comparison with other aptamers, Nucleic Acid Therapeut. 22 (2012) 162–176, https://doi.org/10.1089/nat.2011.0327.
[36] S. Shigdar, J. Macdonald, M. O'Connor, T. Wang, D. Xiang, H. Al Shamaileh, L. Qiao, M. Wei, S.-F. Zhou, Y. Zhu, L. Kong, S. Bhattacharya, C. Li, W. Duan, Aptamers as theranostic agents: modifications, serum stability and functionalisation, Sensors 13 (2013) 13624–13637, https://doi.org/10.3390/s131013624.
[37] S.C.B. Gopinath, T.S. Misono, K. Kawasaki, T. Mizuno, M. Imai, T. Odagiri, P.K.R. Kumar, An RNA aptamer that distinguishes between closely related human influenza viruses and inhibits haemagglutinin-mediated membrane fusion, J. Gen. Virol. 87 (2006) 479–487, https://doi.org/10.1099/vir.0.81508-0.
[38] S.C.B. Gopinath, P.K.R. Kumar, Aptamers that bind to the hemagglutinin of the recent pandemic influenza virus H1N1 and efficiently inhibit agglutination, Acta Biomater. 9 (2013) 8932–8941, https://doi.org/10.1016/j.actbio.2013.06.016.
[39] S.C.B. Gopinath, K. Kawasaki, P.K.R. Kumar, Selection of RNA-aptamer against human influenza B virus, Nucleic Acids Symp. Ser. 49 (2005) 85–86, https://doi.org/10.1093/nass/49.1.85.
[40] H.-M. Woo, J.-M. Lee, S. Yim, Y.-J. Jeong, Isolation of single-stranded DNA aptamers that distinguish influenza virus hemagglutinin subtype H1 from H5, PLoS One 10 (2015), https://doi.org/10.1371/journal.pone.0125060 e0125060.
[41] C. Bai, Z. Lu, H. Jiang, Z. Yang, X. Liu, H. Ding, H. Li, J. Dong, A. Huang, T. Fang, Y. Jiang, L. Zhu, X. Lou, S. Li, N. Shao, Aptamer selection and application in multivalent binding-based electrical impedance detection of inactivated H1N1 virus, Biosens. Bioelectron. 110 (2018) 162–167, https://doi.org/10.1016/j.bios.2018.03.047.
[42] D.S. Reichmuth, S.K. Wang, L.M. Barrett, D.J. Throckmorton, W. Einfeld, A.K. Singh, Rapid microchip-based electrophoretic immunoassays for the detection of swine influenza virus, Lab Chip 8 (2008) 1319, https://doi.org/10.1039/b801396a.
[43] E. Suenaga, P.K.R. Kumar, An aptamer that binds efficiently to the hemagglutinins of highly pathogenic avian influenza viruses (H5N1 and H7N7) and inhibits hemagglutinin–glycan interactions, Acta Biomater. 10 (2014) 1314–1323, https://doi.org/10.1016/j.actbio.2013.12.034.
[44] R. Wang, J. Zhao, T. Jiang, Y.M. Kwon, H. Lu, P. Jiao, M. Liao, Y. Li, Selection and characterization of DNA aptamers for use in detection of avian influenza virus H5N1, J. Virol. Meth. 189 (2013) 362–369, https://doi.org/10.1016/j.jviromet.2013.03.006.
[45] V.-T. Nguyen, H. Bin Seo, B.C. Kim, S.K. Kim, C.-S. Song, M.B. Gu, Highly sensitive sandwich-type SPR based detection of whole H5Nx viruses using a pair of aptamers, Biosens. Bioelectron. 86 (2016) 293–300, https://doi.org/10.1016/J.BIOS.2016.06.064.